Resonance Raman View of Pericyclic Photochemical Ring-Opening Reactions: Beyond the Woodward–Hoffmann Rules

MARY K. LAWLESS,[†] STEVEN D. WICKHAM, AND RICHARD A. MATHIES*

Department of Chemistry, University of California, Berkeley, California 94720

Introduction

Pericyclic rearrangements, which include such diverse reactions as electrocyclic ring-openings and cycloreversions, cycloadditions, sigmatropic shifts, and elimination reactions, have received considerable experimental[1–9] and theoretical[2,10–18] attention over the past 30 years. These reactions are termed pericyclic because they are traditionally described with a transition state having a closed loop of interacting orbitals. The discovery that the stereochemical outcome of pericyclic reactions is dependent on whether the reaction is photochemically or thermally induced was a landmark for physical organic chemistry. This observation catalyzed the development of theories based on orbital symmetry conservation which successfully predict the structural outcome of thermal rearrangements and to a somewhat lesser degree the photochemical reactions.[2,10,11] These predictions, known collectively as the Woodward–Hoffmann rules, provide a framework for understanding the outcome of a plethora of pericyclic reactions. While identical predictions are obtained using a variety of theoretical approaches such as transition-state aromaticity and frontier orbital theory,[13–18] it is the Woodward–Hoffmann rules that have been most widely applied by organic chemists, and we will initially discuss our results in these terms. Advances in laser spectroscopy are now making it possible to directly study the mechanism of a wide variety of photochemical reactions.[19] This raises the intriguing possibility of directly examining the molecular mechanism and transition states involved in pericyclic photochemical reactions. The purpose of this Account is to summarize our recent work on these reactions using resonance Raman spectroscopy, which has allowed us to go beyond the predictive theories and develop an experimentally based description of the actual photochemical pathway of one important class of pericyclic reactions, electrocyclic ring-openings.

Mary K. Lawless was born in Pittsburgh, PA, on September 24, 1965. She received a B.S. in chemistry at St. Edward's University in Austin, TX, in 1987 and a Ph.D. in physical chemistry from the University of California at Berkeley, CA, in 1993. She currently holds a postdoctoral research position at Trimeris, Inc., in Durham, NC, where she is studying peptide and protein structure as it applies to virus fusion mechanisms.

Steven D. Wickham was born in Oneonta, NY, on March 25, 1968. He received a B.S. in chemistry at Ithaca College in Ithaca, NY, in 1989. He is currently pursuing his Ph.D. in physical chemistry at the University of California at Berkeley, where he is continuing his work presented in this Account.

Richard A. Mathies was born in Seattle, WA, on September 20, 1946. He received the B.S. degree in chemistry at the University of Washington in 1968 and a Ph.D. in 1974 from Cornell University in Ithaca, NY. He was a Helen Hay Whitney postdoctoral fellow at Yale University and has been at the University of California at Berkeley since 1976, working on mechanisms of condensed-phase photochemistry and photobiology.

In electrocyclic ring-opening reactions, the structural change occurs through the reorganization of π-bonds accompanied by the breaking of a σ-bond.[11] The reaction stereochemistry is defined by examining the respective rotation of the CH_2 groups on the saturated portion of the ring. As illustrated in Figure 1 for cyclobutene, a conrotatory twisting of the CH_2 groups preserves the C_2 axis of symmetry, whereas a disrotatory twisting of the CH_2 groups preserves the mirror plane of symmetry that bisects the molecular plane. The Woodward–Hoffmann rules predict that, for reactants containing $4n$ π-electrons, the photochemical ring-opening will proceed with conrotatory specificity, while for reactants with $4n + 2$ π-electrons, the photochemical ring-opening will proceed with disrotatory specificity. Thus, as shown in Figure 1, the photochemical ring–opening reactions of cyclobutene (CB) and 1,3,5-cyclooctatriene (COT) are predicted to occur with a disrotatory twisting of the CH_2 groups, while that of 1,3-cyclohexadiene (CHD) occurs with a conrotatory motion. It should be noted, however, that only in the case of cyclohexadiene has the predicted stereochemistry been experimentally confirmed using product analysis of alkyl-substituted CHD.[1,20] The stereochemistry of the photochemical ring-opening of COT has never been investigated to

* To whom correspondence and reprint requests should be addressed.
† Current address: Trimeris, Inc., 4727 University Drive, Durham, NC 27707.
(1) De Kock, R. J.; Minnaard, N. G.; Havinga, E. *Recl. Trav. Chim. Pays-Bas* **1960**, *79*, 922–934.
(2) Havinga, E.; Schlatmann, J. L. M. A. *Tetrahedron* **1961**, *16*, 146–152.
(3) Fonken, G. J. *Tetrahedron Lett.* **1962**, 549–551.
(4) Lewis, K. E.; Steiner, H. *J. Chem. Soc.* **1964**, 3080–3092.
(5) Adam, W. *Chem. Ber* **1964**, *97*, 1811–1817.
(6) Criegee, R.; Furrer, H. *Chem. Ber.* **1964**, *97*, 2949–2952.
(7) Crowley, K. J. *J. Org. Chem.* **1968**, *33*, 3679–3686.
(8) Dauben, W. G.; McInnis, E. L.; Michno, D. M. Photochemical Rearrangements in Trienes. In *Rearrangements in Ground and Excited States*; de Mayo, P., Ed.; Academic Press: New York, 1980; pp 91–129.
(9) Jacobs, H. J. C.; Havinga, E. Photochemistry of Vitamin D and Its Isomers and of Simple Trienes. In *Advances in Photochemistry*; Pitts, J. N., Jr., Hammond, G. S., Gollnick, K., Eds.; Interscience Publishers: New York, 1979; pp 305–373.
(10) Longuet-Higgins, H. C.; Abrahamson, E. W. *J. Am. Chem. Soc.* **1965**, *87*, 2045–2046.
(11) Woodward, R. B.; Hoffmann, R. *The Conservation of Orbital Symmetry*; Verlag Chemie: Weinheim/Deerfield Beach, 1970.
(12) Fukui, K. *Acc. Chem. Res.* **1971**, *4*, 57–64.
(13) Dewar, M. J. S. *Angew. Chem., Int. Ed. Engl.* **1971**, *10*, 761–870.
(14) Zimmerman, H. E. *Tetrahedron* **1982**, *38*, 753–758.
(15) van der Lugt, W. T.; Oosterhoff, L. J. *J. Chem. Soc., Chem. Commun.* **1968**, 1235–1236.
(16) Mulder, J. J. C.; Oosterhoff, L. J. *J. Chem. Soc., Chem. Commun.* **1970**, 307–309.
(17) van der Hart, W. J.; Mulder, J. J. C.; Oosterhoff, L. J. *J. Am. Chem. Soc.* **1972**, *94*, 5724–5731.
(18) Fukui, K. *Angew. Chem., Int. Ed. Engl.* **1982**, *21*, 801–876.
(19) Femtosecond Chemistry: The Berlin Conference issue of *J. Phys. Chem.* **1993**, *97*, 12423–12650.
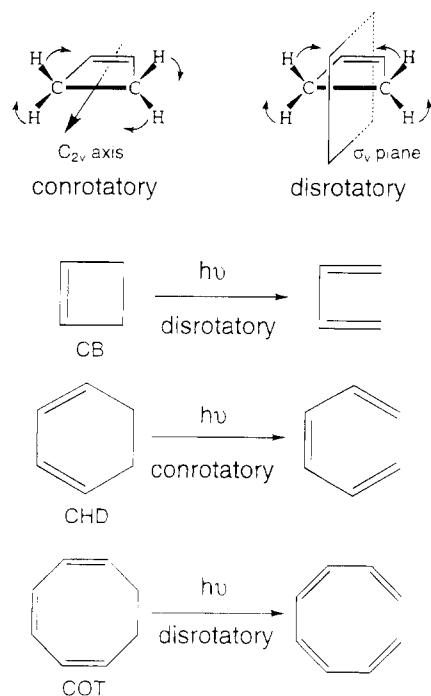
Figure 1. Top structures depict the conrotatory (thermal) and disrotatory (photochemical) ring openings of CB. Lower structures summarize the predicted photochemical ring-opening reactions of CB, CHD, and COT.

Figure 2. Orbital symmetry correlation diagrams for the photochemical ring opening of CB. The σ- and π-bonding orbitals are ordered in energy and labeled symmetric (S) or antisymmetric (A) with respect to the symmetry element being preserved. Conrotatory motion produces a symmetry-imposed barrier, while disrotatory motion gives rise to a barrierless transition to the product.

our knowledge, but its primary photoproduct is known to be 1,3,5,7-octatetraene.[21] For CB, alkyl substitutions have produced mixtures of both forbidden and allowed photoproducts with the relative amounts sometimes favoring the forbidden product.[22] However, alkyl substitutions can significantly change the ordering and interactions of electronic states involved in the photochemical dynamics through inductive or hyperconjugative mechanisms,[23] and they introduce significant steric and mass perturbations.

The chemical basis of the Woodward–Hoffmann predictions has been traditionally understood by examining molecular orbital correlation diagrams.[10,11,24] For example, Figure 2 presents the correlation diagram for cyclobutene for both the conrotatory and disrotatory photochemical pathways. Starting with the approximate electronic configuration for the one-electron excited state, a symmetry-imposed barrier arises as the conrotatory photochemical ring-opening proceeds. On the other hand, no symmetry-imposed barrier arises for the disrotatory photochemical ring-opening motion. Thus, the photochemical ring-opening reaction of CB should involve a disrotatory motion of the CH_2 groups.

Although many aspects of electrocyclic reactions have been explored,[25-36] it has only recently been

possible for us to directly examine their excited-state reaction dynamics.[37-44] In these studies we have addressed a number of fundamental questions about

(20) (a) Baldwin, J. E.; Krueger, S. M. *J. Am. Chem. Soc.* **1969**, *91*, 6444. (b) Dauben, W. G.; Rabinowitz, J.; Vietmeyer, N. D.; Wendschuh, P. H.; *J. Am. Chem. Soc.* **1972**, *94*, 4285. (c) Spangler, C. W.; Hennis, R. P. *J. Chem. Soc., Chem. Commun.* **1972**, 24.

(21) (a) Houssain, M.; Kohler, B. E.; West, P. *J. Phys. Chem.* **1982**, *86*, 4918. (b) Goldfarb, T. D.; Lindqvist, L. *J. Am. Chem. Soc.* **1967**, *89*, 4588. (c) Datta, P.; Goldfarb, T. D.; Boikess, R. S. *J. Am. Chem. Soc.* **1969**, *91*, 5429.

(22) Leigh, W. J. *Can. J. Chem.* **1993**, *71*, 147 and references within.

(23) Dinur, U.; Honig, B. *J. Am. Chem. Soc.* **1979**, *101*, 4453–4460.

(24) A proper analysis of the chemical reaction pathways must employ the correlation diagrams for the electronic states, as will be discussed in detail below. However, the molecular orbital correlation diagrams provide a useful qualitative understanding of the stereospecificity of the bonding changes.
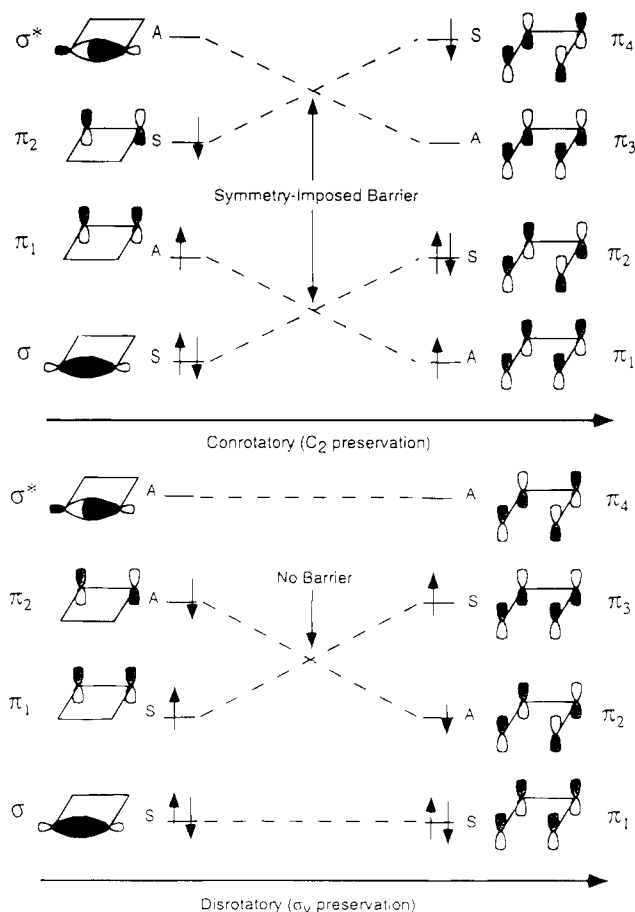
(25) Michl, J. *Mol. Photochem.* **1972**, *4*, 287–314.

(26) Berson, J. A. *Acc. Chem. Res.* **1972**, *5*, 406–414.

(27) Baldwin, J. E.; Andrist, A. H.; Pinschmidt, R. K., Jr. *Acc. Chem. Res.* **1972**, *5*, 402–406.

(28) Goddard, W. A., III *J. Am. Chem. Soc.* **1972**, *94*, 793–807.

(29) Gilchrist, T. L.; Storr, R. C. *Organic Reactions and Orbital Symmetry*; University Press: Cambridge, 1972.

(30) Silver, D. M. *J. Am. Chem. Soc.* **1974**, *96*, 5959–5967.

(31) Halevi, E. A. *Angew. Chem., Int. Ed. Engl.* **1976**, *15*, 593–607.

(32) Lehr, R. E.; Marchand, A. P. Operational Criteria for Evaluation of Concertedness in Potential Pericyclic Reactions. In *Pericyclic Reactions*; Marchand, A. P., Lehr, R. E., Eds.; Academic Press: New York, 1977; pp 1–51.

(33) Metiu, H.; Ross, J.; Whitesides, G. M. *Angew. Chem., Int. Ed. Engl.* **1979**, *18*, 377–392.

(34) Epiotis, N. D.; Shaik, S.; Zander, W. Rearrangements: A Theoretical Approach. In *Rearrangements in Ground and Excited States*; de Mayo, P., Ed.; Academic Press: New York, 1980; pp 1–94.

(35) Ponec, R.; Strnad, M. *Int. J. Quantum Chem.* **1992**, *42*, 501–508.

(36) Squire, A. E.; Squire, R. H. *Int. J. Quantum Chem.* **1992**, *43*, 481–510.

(37) Trulson, M. O.; Dollinger, G. D.; Mathies, R. A. *J. Am. Chem. Soc.* **1987**, *109*, 586–587.

(38) Trulson, M. O.; Dollinger, G. D.; Mathies, R. A. *J. Chem. Phys.* **1989**, *90*, 4274–4281.

(39) Reid, P. J.; Doig, S. J.; Mathies, R. A. *Chem. Phys. Lett.* **1989**, *156*, 163–168.

(40) Reid, P. J.; Doig, S. J.; Mathies, R. A. *J. Phys. Chem.* **1990**, *94*, 8396–8399.

(41) Reid, P. J.; Doig, S. J.; Wickham, S. D.; Mathies, R. A. *J. Am. Chem. Soc.* **1993**, *115*, 4754–4763.

(42) Lawless, M. K.; Mathies, R. A. *J. Chem. Phys.* **1994**, *100*, 2492.

these reactions: What nuclear dynamics make up the reaction coordinate? When is the stereochemistry established? What excited states participate in these reactions? Is only one excited electronic state responsible for the photochemistry, as implied by the Woodward–Hoffmann rules? And lastly, how fast do these photochemical reactions occur?

We have answered many of these questions regarding the photodynamics of electrocyclic ring-opening reactions by using resonance Raman spectroscopy.[37,38,42,43] A previous review provided an overview of the use of both picosecond time-resolved resonance Raman and resonance Raman intensity analysis to examine pericyclic reaction dynamics.[44] Here we will focus on the use of resonance Raman intensity analysis to examine the excited-state dynamics of organic photochemical reactions and specifically compare the ring-opening dynamics obtained for differing ring sizes. Information on the excited-state geometry changes for pericyclic photochemical reactions is difficult to obtain by traditional techniques because these systems have very broad and unresolved near-UV absorption spectra in both solution and gas phases, and diminutive (10^{-6}) fluorescence quantum yields.[38,42,45,46] However, resonance Raman spectroscopy can be used to extract a great deal of information about chemical reaction dynamics even in such cases. To obtain mode-specific information on nuclear motions that occur in the first femtoseconds after optical excitation, we exploit the dependence of the resonance Raman intensities on the properties of the excited-state potential energy surface.[47,48] This technique has proven useful for examining excited-state structure and dynamics in a variety of chemical and biological systems.[46,49–62] Here we show that resonance Raman intensities can be used to determine the initial excited-state nuclear dynamics in photochemical electrocyclic

reactions. This work has provided a direct picture of the nuclear dynamics that initiate these reactions and has led to a fundamental new understanding of the states involved.

Resonance Raman Intensity Analysis: Our Photodynamics Viewing Tool

Photochemical reactions occur because a molecule's nuclear framework evolves under the influence of the altered excited-state electronic potential. This nuclear evolution can be described as a combination of motions along the individual normal modes. Therefore, mode-specific knowledge of the geometry changes that occur upon electronic excitation reveals how the molecule begins its journey from reactant to product. For symmetric modes, the difference in the equilibrium geometries between the ground and excited states along a particular normal mode (denoted as Δ in Figure 3) is the primary piece of information gained from fundamental resonance Raman intensities. Central to resonance Raman intensity analysis is the dependence of both the absorption spectrum and the resonance Raman intensities on the same molecular parameters; this permits the modeling of the experimental spectra with a single set of parameters describing the excited-state potential surface. By carefully measuring the resonance Raman intensity of each symmetric vibrational mode, we can determine how the excited-state geometry differs from that of the ground state. In addition, the intensities of nontotally symmetric overtones permit the description of frequency changes along those coordinates (see below).

The most intuitive description of the connection between primary molecular parameters (Δ's) and the resonance Raman and absorption cross sections (intensities) is given by the time-dependent theory of resonance Raman scattering presented in eqs 1 and 2 and in Figure 3.[63–65] The molecular potential surface, illustrated in Figure 3 for one vibrational coordinate, is described by ground- and excited-state harmonic potentials, displaced vertically by the zero–zero energy and horizontally by a dimensionless displacement Δ, which quantitates the change in equilibrium geometry between the ground and excited electronic potentials.[66,67]

$$\sigma_R(E_L) =$$
$$\frac{8\pi e^4 E_S{}^3 E_L M^4}{9\hbar^6 c^4}|\int_0^\infty \langle f|i(t)\rangle e^{i(E_L+\epsilon_i)t/\hbar} e^{-\Gamma^2 t^2/\hbar^2}\, dt|^2 \quad (1)$$

$$\sigma_A(E_L) = \frac{4\pi e^2 E_L M^2}{6\hbar^2 cn}\int_{-\infty}^{\infty} \langle i|i(t)\rangle e^{i(E_L+\epsilon_i)t/\hbar} e^{-\Gamma^2 t^2/\hbar^2}\, dt \quad (2)$$

In eqs 1 and 2, E_L and E_S are the energies of the incident and scattered photons, M is the solution-

(43) Lawless, M. K.; Wickham, S. D.; Mathies, R. A. *J. Am. Chem. Soc.* **1994**, *116*, 1593.

(44) Reid, P. J.; Lawless, M. K.; Wickham, S. D.; Mathies, R. A. *J. Phys. Chem.* **1994**, *98*, 5597.

(45) Minnaard, N. G.; Havinga, E. *Recl. Trav. Chim. Pays-Bas* **1973**, *92*, 1179.

(46) Reid, P. J.; Shreve, A. P.; Mathies, R. A. *J. Phys. Chem.* **1993**, *97*, 12691–12699.

(47) Myers, A. B.; Mathies, R. A. *Resonance Raman Intensities: A Probe of Excited-State Structure and Dynamics.* In *Biological Applications of Raman Spectrometry*; Spiro, T. G., Ed.; Wiley-Interscience: New York, 1987; pp 1–58.

(48) Lawless, M. K.; Reid, P. J.; Mathies, R. A. Analysis of Condensed Phase Photochemical Reaction Mechanisms with Resonance Raman Spectroscopy. In *Ultrafast Dynamics of Chemical Systems*; Simon, J. D., Ed.; Kluwer Academic Publishers: The Netherlands, 1994; pp 267–287.

(49) Sension, R. J.; Strauss, H. L. *J. Chem. Phys.* **1988**, *88*, 2289–2295.

(50) Butler, L. J. *Chem. Phys. Lett.* **1991**, *182*, 393–399.

(51) Ziegler, L. D.; Hudson, B. S. *J. Chem. Phys.* **1983**, *79*, 1197–1202.

(52) Trulson, M. O.; Mathies, R. A. *J. Phys. Chem.* **1990**, *94*, 5741–5747.

(53) Phillips, D. L.; Zgierski, M. Z.; Myers, A. B. *J. Phys. Chem.* **1993**, *97*, 1800–1809.

(54) Ci, X.; Myers, A. B. *Chem. Phys. Lett.* **1989**, *158*, 263–270.

(55) Ziegler, L. D.; Hudson, B. S. *J. Chem. Phys.* **1983**, *79*, 1134–1137.

(56) Shin, K.-S.; Clark, R. J. H.; Zink, J. I. *J. Am. Chem. Soc.* **1989**, *111*, 4244–4250.

(57) Peteanu, L. A.; Mathies, R. A. *J. Phys. Chem.* **1992**, *96*, 6910–6916.

(58) Blazej, D. C.; Peticolas, W. L. *J. Chem. Phys.* **1980**, *72*, 3134–3142.

(59) Stallard, B. R.; Callis, P. R.; Champion, P. M.; Albrecht, A. C. *J. Chem. Phys.* **1984**, *80*, 70–82.

(60) Loppnow, G. R.; Mathies, R. A. *Biophys. J.* **1988**, *54*, 35–43.

(61) Schomacker, K. T.; Champion, P. M. *J. Chem. Phys.* **1989**, *90*, 5982–5993.

(62) Sweeney, J. A.; Asher, S. A. *J. Phys. Chem.* **1990**, *94*, 4784–4791.

(63) Lee, S.-Y.; Heller, E. J. *J. Chem. Phys.* **1979**, *71*, 4777–4788.

(64) Heller, E. J.; Sundberg, R. L.; Tannor, D. *J. Phys. Chem.* **1982**, *86*, 1822–1833.

(65) Tannor, D. J.; Heller, E. J. *J. Chem. Phys.* **1982**, *77*, 202–218.

(66) Tang, J.; Albrecht, A. C. Developments in the Theories of Vibrational Raman Intensities. In *Raman Spectroscopy*; Szymanski, H. A., Ed.; Plenum Press: New York, 1970; pp 33–67.

(67) The totally symmetric modes may also experience a frequency change in the excited state that can be described by somewhat more complicated forms of the time-dependent equations. However, for strongly displaced symmetric modes the fundamental and overtone intensities will be dominated by the effect of Δ.
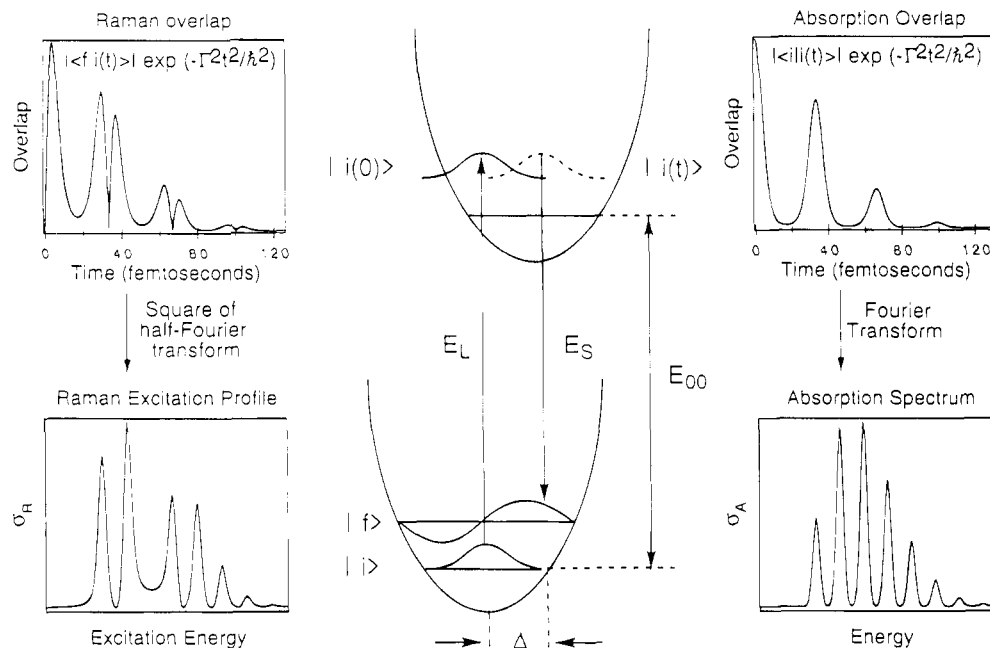
Figure 3. Schematic of the time-dependent picture of resonance Raman scattering and absorption. Interaction of the incident photon with the molecule through the electronic transition moment creates a virtual wavepacket $|i(t)\rangle$ that evolves under the influence of the excited-state vibrational Hamiltonian. The Raman cross section as a function of the incident photon energy E_L is given by the square of the half Fourier transform of the time-dependent overlap between $|i(t)\rangle$ and the final vibrational level $|f\rangle$. The absorption spectrum is given by the full Fourier transform of the time-dependent overlap between $|i(t)\rangle$ and the initial ground vibrational state $|i\rangle$.

phase electronic transition moment, ϵ_i is the energy of the initial vibrational level, n is the solvent refractive index, and Γ is the homogeneous line width. The initial and final ground-state vibrational wave functions in the Raman process are $|i\rangle$ and $|f\rangle$; and $|i(t)\rangle$ is the initial ground-state nuclear wave function propagated on the excited-state potential surface.[68-70] At the heart of these equations are the correlation functions $\langle f|i(t)\rangle$ and $\langle i|i(t)\rangle$. These functions are the time-dependent overlaps of the excited-state wavepacket, $|i(t)\rangle$, with the final ground-state vibrational wavefunction, $|f\rangle$, or with the initial ground-state wave function, $|i\rangle$. These time-dependent overlaps for the Raman and absorption processes are depicted in Figure 3 for a single vibrational mode. Also shown in Figure 3 are the Raman cross sections for varying excitation wavelength, generated by squaring the half Fourier transform of $\langle f|i(t)\rangle$, and the absorption cross sections, generated by Fourier transforming $\langle i|i(t)\rangle$. Immediately after virtual excitation, the Raman overlap $\langle f|i(t)\rangle$ is zero due to the orthogonality of $|i(0)\rangle$ and $|f\rangle$. If there is no difference in equilibrium geometry between the two excited states ($\Delta = 0$), the wavepacket will not move from the Franck–Condon region, $\langle f|i(t)\rangle$ will not grow from zero, and no resonance Raman intensity will be generated. However, when there is a displacement, the wavepacket $|i(t)\rangle$ will move away from the Franck–Condon region and oscillate around the new equilibrium geometry. The amplitude of the overlap is damped by the homogeneous damping function. As the integrated area of $\langle f|i(t)\rangle$ is increased by increasing the displacement, the integrated area of the Raman excitation profile (REP) will increase.

Therefore, if one observes strong resonance Raman intensity in a particular symmetric vibrational mode, it is immediately clear that there is a substantial displacement along that mode. It is this intimate connection between the Δ's and the resonance Raman intensities that makes resonance Raman such a powerful tool for understanding the initial stages of nuclear motion in photochemical reactions.

Non-totally symmetric vibrations derive resonance Raman activity through more complicated mechanisms. The potential surface depicting one possible mechanism is presented in Figure 4. If the molecule maintains its symmetry, there can be no equilibrium geometry change along a non-totally symmetric coordinate, and therefore these modes cannot exhibit fundamental resonance Raman intensity. However, if the excited-state frequency is lower (or higher) than that of the ground state, $|i(t)\rangle$ will respond by spreading (or compressing) along this coordinate, resulting in overlap between $|i(t)\rangle$ and the final vibrational wave functions corresponding to even overtone resonance Raman scattering ($|f\rangle = |2\rangle$, $|4\rangle$, ...).[64] This can also provide important information about the excited-state potential surface for photochemical systems as will be discussed below for CB. In addition, non-totally symmetric modes can give rise to resonance Raman activity through vibronic coupling mechanisms known as B-term scattering,[67] but this scattering will generally be weaker than the mechanisms considered here.

For real molecular systems $\langle f|i(t)\rangle$ is a multimode correlation function that is written as the product of $\langle f|i(t)\rangle$ for the Raman active mode and $\langle i|i(t)\rangle$ for the remaining $3N - 7$ vibrational modes. The multimode correlation function $\langle i|i(t)\rangle$ in the absorption cross section is simply the product of the $\langle i|i(t)\rangle$'s for all vibrational modes. The multimode nature of these overlaps is an important consideration in Raman cross

(68) Within the harmonic approximation, the values of the overlaps $\langle i|i(t)\rangle$ and $\langle f|i(t)\rangle$ are known and can be calculated analytically (refs 47 and 69).

(69) Manneback, C. *Physica* **1951**, *17*, 1001–1010.

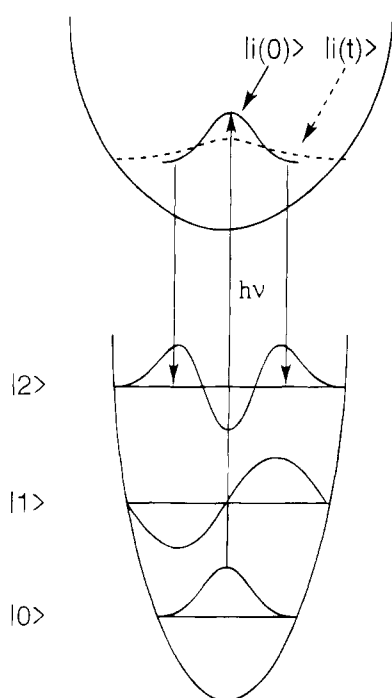(70) Heller, E. J. *J. Chem. Phys.* **1975**, *62*, 1544–1555.

Pericyclic Photochemical Ring-Opening Reactions

Acc. Chem. Res., Vol. 28, No. 12, 1995 **497**

Figure 4. Overtone scattering by a non-totally symmetric mode can arise from a change of frequency in the excited state. The figure depicts an example in which the excited-state potential softens to give a lower excited-state frequency.

section calculations since strong Franck–Condon activity in one mode can damp the multimode Raman overlap $\langle f|i(t)\rangle$ *for a second mode* and, hence, the resonance Raman intensity in that second mode.[47]

The homogeneous decay function $\exp(-\Gamma^2 t^2/\hbar^2)$ also damps the oscillations of the correlation functions and represents any phase-disrupting process that destroys the vibronic overlap present at $t = 0$. The $1/e$ time constant of this function is the optical T_2. It includes contributions from both T_1 (electronic and vibrational energy relaxation) and T_2^* (pure vibronic dephasing processes.[71] The homogeneous damping function is normally taken to be an exponential. However, for the systems reported in this Account and several others studied in our laboratory, the Gaussian damping function presented in the equations provides a better description of the ultrashort dephasing times that are observed.[38,52,72]

Resonance Raman Investigations of Photochemical Ring-Opening Reactions

Cyclobutene. The electrocyclic ring-opening reaction of cyclobutene is predicted to occur with a non totally symmetric disrotatory motion of the CH_2 groups. Figure 5 presents the resonance Raman spectrum of CB excited at 200 nm.[43] The strongest vibrational band is the 1563 cm^{-1} C=C stretching mode indicative of the expected increase in bond length along this coordinate upon electronic excitation. Strong intensity in the 1110 cm^{-1} aliphatic CH_2–CH_2 stretch is also observed, consistent with the fact that this bond breaks during the course of the photochemical reaction. Importantly, the symmetric CH_2 scissors mode at 1440 cm^{-1} parallels the change in hybridiza-

(71) Zewail, A. H. *Acc. Chem. Res.* **1980**, *13*, 360–368.
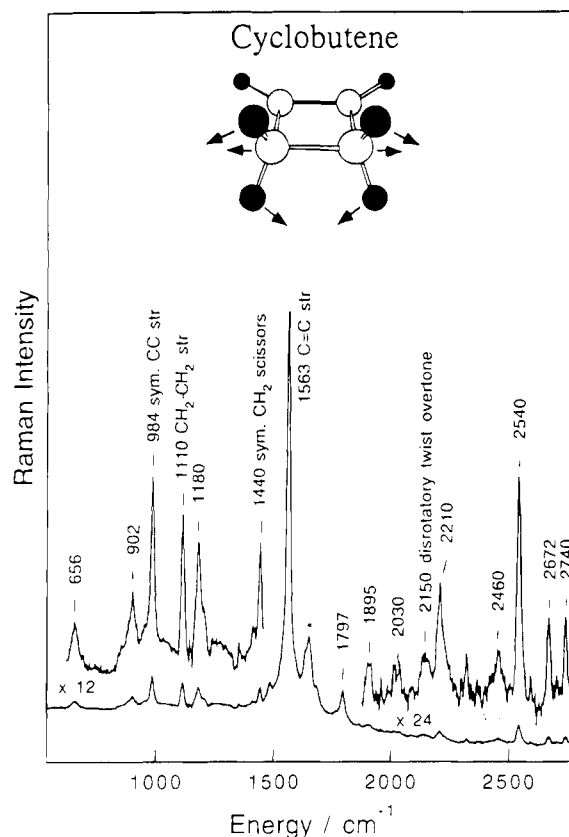(72) Lawless, M. K.; Mathies, R. A. *J. Chem. Phys.* **1992**, *96*, 8037–8045.

Figure 5. Resonance Raman spectrum of CB obtained with 200 nm excitation. The inset depicts the ground-state geometry of CB with arrows illustrating the direction of geometry changes that occur ∼30 fs after excitation as a result of evolution along the CH_2–CH_2 stretch and disrotatory CH_2 twist modes. Adapted from ref 43.

tion of the methylene carbons as the CH_2–CH_2 bond breaks: the HCH bond angle must change from 109° for CB to 120° for 1,3-butadiene. The symmetric CH_2 twisting mode at 1145 cm^{-1} is not observed, indicating that no initial evolution occurs along the conrotatory reaction coordinate. The fundamental of the non-totally symmetric CH_2 twist mode is also not observed, as expected by symmetry. More interestingly, significant intensity is observed for the overtone of the non-totally symmetric CH_2 twist at 2150 cm^{-1} indicating that a frequency reduction of ∼200 cm^{-1} has occurred along this coordinate. This mode projects directly onto the disrotatory twist of the CH_2 groups, indicating that evolution along this reactive coordinate occurs directly out of the Franck–Condon region via a decrease in the excited-state frequency of this mode.[73] *The observed intensity of the CH_2 twist supports the idea that the stereochemical preference for the Woodward–Hoffmann predicted disrotatory geometry change is established in the Franck–Condon region.* This is depicted in the inset to Figure 5, where the arrows give the geometry changes that occur ∼30 fs after excitation as a result of evolution along the CH_2–CH_2 stretch and CH_2 twist normal modes.

(73) The observed overtone intensity for the non-totally symmetric twist mode in CB could be accounted for by either an increase or a decrease in the excited-state frequency. However, on the basis of the reactive nature of this system we have assumed that there is a decrease. Although the observed frequency change is not sufficient to make the excited state unbound about this coordinate, once the system moves further from the Franck–Condon region, enhanced changes of the electronic structure are likely to occur (see below).
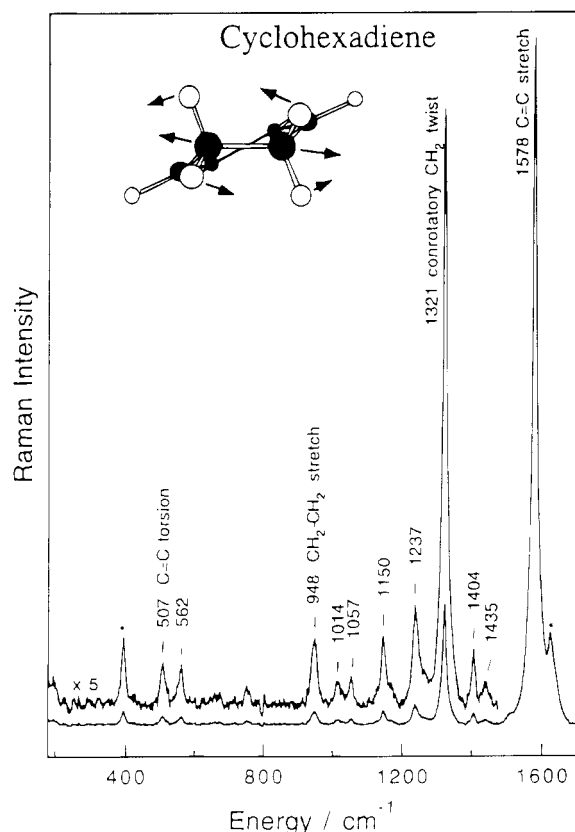
Figure 6. Resonance Raman spectrum of CHD in cyclohexane obtained with 257 nm excitation. The inset presents the ground-state geometry of CHD with arrows depicting geometry changes of the saturated portion of the ring (multiplied 20-fold) that occur ~10 fs after excitation as a result of evolution along all the displaced normal modes. Adapted from ref 38.

Cyclohexadiene. The resonance Raman spectrum of cyclohexadiene excited at 257 nm is presented in Figure 6.[37,38] As expected for a $\pi-\pi^*$ transition, this spectrum is dominated by intense scattering in the normal modes corresponding to the symmetric C=C stretch (1578 cm^{-1}). We also observe enhancement of the 948 cm^{-1} CH$_2$–CH$_2$ single bond stretching mode, indicating that this aliphatic bond, which breaks in the course of the reaction, lengthens immediately upon Franck–Condon excitation. It is evident that the σ-skeleton is significantly involved in this nominally $\pi-\pi^*$ excitation. Most striking is the unusually strong intensity of the symmetric CH$_2$ twisting mode at 1321 cm^{-1}.[37,38] *The observation of intense scattering in both the CH₂–CH₂ stretch and the symmetric CH₂ twist modes reveals that the nuclear dynamics that occur immediately after excitation, project directly onto the conrotatory ring-opening reaction coordinate. The stereochemistry of this reaction is clearly established in the Franck–Condon region.* The absolute resonance Raman intensities of CHD determined by Trulson et al.[38] establish the magnitude of the geometry changes along both the CH$_2$–CH$_2$ stretch (0.05 Å) and the CH$_2$ twist modes (5°) based on a harmonic approximation. The arrows in Figure 6 present the atomic motions that occur for CHD along the combination of these two modes after ~10 fs of propagation on the excited-state surface.

If the stereochemical preferences are established for CB and CHD by the optically prepared excited state, it is important to get some measure of how long the
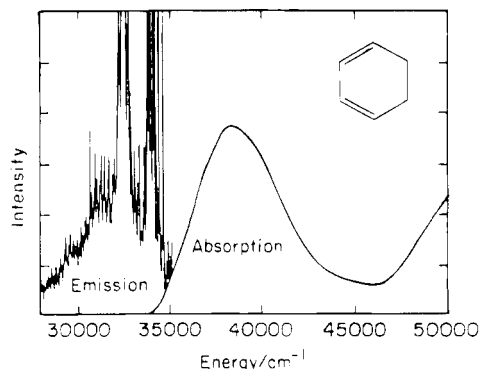

Figure 7. Absorption and emission spectra of CHD obtained with 282 nm excitation. Adapted from ref 38.

molecules evolve on this surface. Basic information on the initial excited-state lifetime can be obtained by measuring the total fluorescence quantum yield.[38,42,46,74] This approach was first applied to CHD. Figure 7 presents the absorption and emission spectra for CHD excited at 282 nm. The measured fluorescence quantum yield of 2 × 10^{-6} can be compared with the natural radiative lifetime that is calculated from the optical absorption spectrum. This calculation reveals that the optical lifetime (T_1) or depopulation of the initially prepared excited state for CHD is on the time scale of 10 fs. This indicates that there is a very rapid internal conversion process that depopulates the initially prepared excited state of CHD. Very similar conclusions have been presented for CB.[43]

Cyclooctatriene. The resonance Raman spectrum of 1,3,5-cyclooctatriene excited at 257 nm is presented in Figure 8. This spectrum is dominated by intense C=C stretches which lie at 1610 and 1640 cm^{-1}. These two modes correspond to different combinations of the three individual C=C bonds; the in-phase (+++ combination) mode lies at 1610 cm^{-1}, while the out-of-phase (+–+ combination) lies at 1640 cm^{-1}. As expected from symmetry rules, fundamental intensity in the mode corresponding to the 1356 cm^{-1} non totally symmetric disrotatory CH$_2$ twist does not appear. Evidence for softening of the potential surface about the disrotatory CH$_2$ twist would be revealed by even overtone intensity of this mode as we observed for CB. However, all modes in the overtone region of the spectrum can be assigned to combinations of the two ethylenics with the remaining observed modes in the fundamental spectrum. *There is no evidence for reactive motion out of the Franck–Condon region.* So what molecular geometry changes do occur after electronic excitation? Interestingly, very intense modes are observed in the low-frequency (100–400 cm^{-1}) portion of the spectrum that are due to skeletal bends and deformations. In particular, the very strong 140 cm^{-1} mode corresponds to planarization of the ground-state twist-boat structure depicted in Figure 8. *These results indicate that there is no detectable evolution along the ring-opening reaction coordinate as COT leaves the Franck–Condon region. Instead the dominant motion is the planarization of the relatively nonplanar twist-boat structure.* A very similar result has been obtained in resonance Raman studies of the [1,7]-hydrogen shift in the seven-membered ring of 1,3,5-cycloheptatriene.[46]

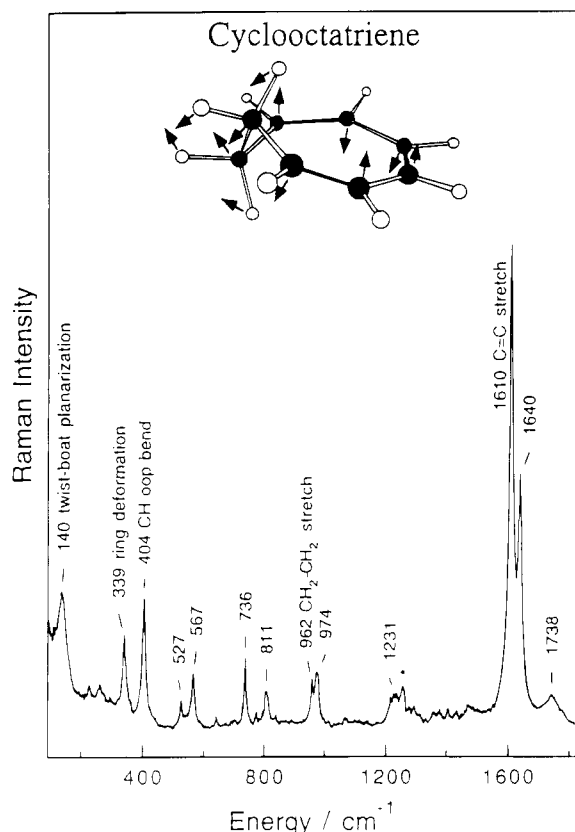(74) Strickler, S. J.; Berg, R. A. *J. Chem. Phys.* **1962**, *37*, 814–822.

Figure 8. Resonance Raman spectrum of COT in cyclohexane obtained with 257 nm excitation. The inset presents the ground-state geometry with arrows depicting the planarization geometry changes that occur after excitation as a result of evolution along all displaced normal modes. Adapted from ref 42.

Discussion

Stereochemical Preferences for Cyclobutene and Cyclohexadiene Are Established in the Franck–Condon Excited State. The initial nuclear dynamics revealed by the resonance Raman spectra of CB and CHD are exactly those predicted by the Woodward–Hoffmann rules. The resonance Raman intensities of CB show that evolution along the disrotatory reaction coordinate commences immediately after optical excitation. Similarly, the resonance Raman intensities of CHD show that the stereochemical preference for the conrotatory reactive motion is established immediately after excitation. Therefore, the nuclear dynamics of CB and CHD demonstrate concerted evolution along their respective reaction coordinates immediately after excitation.

The initial excited states depopulate on a femtosecond time scale while time-resolved resonance Raman spectroscopy has shown that the ground-state photoproducts appear in ~10 ps.[37-41] The very short lifetime of the initially prepared 1B$_2$ excited state measured for these systems makes it clear that the initially prepared excited state plays an important but brief role. Thus, the rest of the photochemical rearrangement must occur on a second excited electronic state that is analogous to the low-lying 2A$_g$ electronic state in linear polyenes.[75] The role of the optically prepared excited state is to direct the excited reactant

toward the region of the potential energy surface where the rest of the pericyclic rearrangement occurs.

Figure 9 presents schematic reaction coordinate models for the conrotatory ring opening of CHD and the disrotatory ring opening of CB. After excitation of CHD, the molecule evolves in a symmetric conrotatory direction accomplishing about 10% of the ring opening. At this point, the allowed crossing of the 1B$_2$ and 2A$_1$ states is reached and a non totally symmetric distortion (not shown) catalyzes the crossing to the 2A$_1$ state on the 10 fs time scale. In the case of CB the initial dynamics are different. The initial excitation is to a saddle point. Non-totally symmetric spreading of the wavepacket carries the system to the crossing between the 1B$_2$ and 2A$_1$ surfaces where direct passage to the lower lying state can continue along the same coordinate since this is an avoided crossing.

Cyclooctatriene: Planarization before Photochemistry. The dominant excited-state nuclear dynamics for COT in the Frank–Condon region are not those predicted by the Woodward–Hoffmann rules. The pattern of resonance Raman intensities for COT is characteristic of a more complicated reaction coordinate, involving planarization of the ring in the first stages of the reaction. This fundamental difference of the excited-state dynamics of COT compared to CB and CHD can be understood by examining the ground-state structures of these molecules. The ground-state structure of the carbon framework of CB (Figure 5) is planar, and that of CHD (Figure 6) is close to planar (~15° C=C−C=C torsional angle). However, COT (Figure 8) is found in a twist-boat form that is significantly distorted from planarity (~63° CH$_2$−CH$_2$ torsional angle).[76] This suggests that the presence of a planar geometric structure is a critical factor in the pericyclic reaction mechanism. No motion along planarization coordinates is required before the reactive motion ensues for CB, and limited skeletal planarization occurs in the excited state of CHD before the reactive changes begin. On the other hand, COT is highly nonplanar, so ring planarization dominates the initial dynamics. This relationship between the ring-flattening modes and the disrotatory ring-opening reaction of COT allows us to construct the three-dimensional reaction-coordinate model in Figure 10. Excitation within the lowest allowed electronic transition leads to the population of the 1B$_2$ electronic state (shown in green). This is followed by evolution along the symmetric ring-planarization coordinate which brings the system to the intersection with the 2A$_1$ electronic state (shown in red). The low fluorescence quantum yield of 2×10^{-6} again indicates that COT experiences very rapid internal conversion that is only consistent with a rapid and efficient crossing to a low-lying 2A$_1$ state. A b$_2$-symmetry distortion, drawn in Figure 10 as the motion along the b$_2$ disrotatory reaction coordinate, couples the system from the 1B$_2$ to the lower 2A$_1$ electronic state where the ring-opening dynamics occur. Subsequent coupling of this electronic state to the ground state (shown in blue) produces the photoproduct in ~12 ps.[40]

Implications for the Mechanism of Pericyclic Reactions. Resonance Raman intensity analysis has thus provided unique mode-specific information about

(75) Hudson, B. S.; Kohler, B. E.; Schulten, K. Linear Polyene Electronic Structure and Potential Surfaces. In *Excited States*; Lim, E. C., Ed.; Academic Press: New York, 1982; pp 1–93.

(76) Anet, F. A. L.; Yavari, I. *Tetrahedron* **1978**, *34*, 2879–2886.
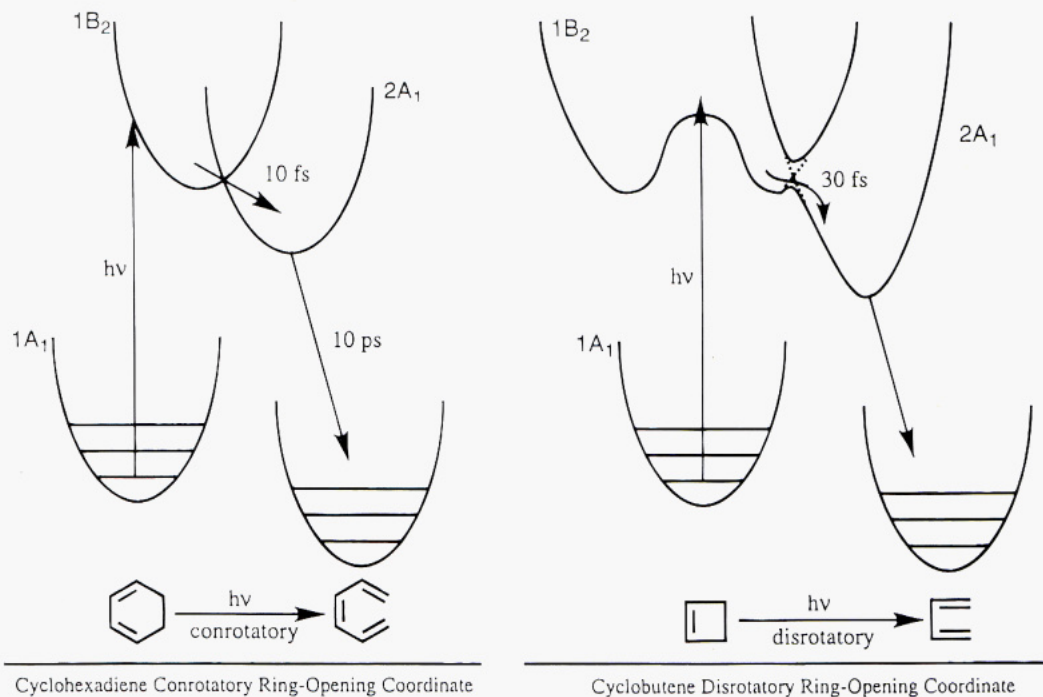
Figure 9. Schematic reaction coordinates for the photochemical ring opening of CHD and CB. The reaction coordinate for CB is depicted with a double well about the disrotatory ring-opening coordinate that corresponds to the two possible directions for the disrotatory twisting motion.
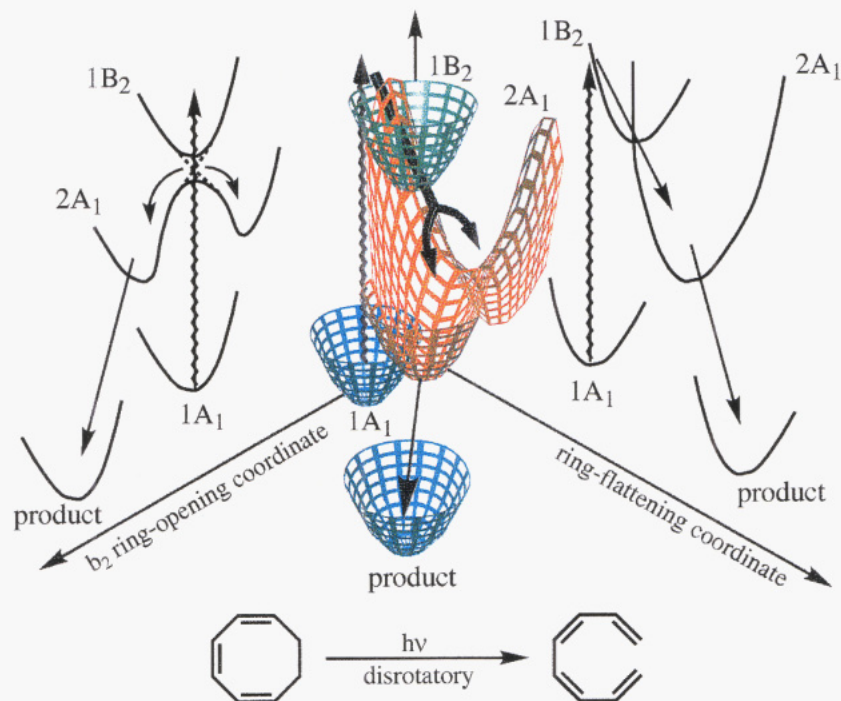

Figure 10. Schematic potential surfaces for the photochemical ring opening of COT. After excitation, the initial motion along the ring-flattening coordinate carries the molecule to a crossing of the $1B_2$ with the $2A_1$ surface. In this region, the two surfaces are coupled by the b_2 disrotatory ring-opening mode. This region of the $2A_1$ potential surface is depicted as a saddle point because the wavepacket will bifurcate along the two possible disrotatory twisting motions. The two-dimensional projections are obtained by slicing through the Franck–Condon region along the ring-flattening coordinate and through the $2A_1$ saddle point along the ring-opening coordinate.

the excited-state nuclear dynamics that initiate pericyclic photochemical reactions. These observations suggest that *a planar or near-planar geometry must be formed before the electronic bonding changes that characterize a pericyclic photochemical reaction can occur.* The nonplanar, ground-state structure of COT does not allow proper orbital overlap between carbons involved in the pericyclic reaction. Thus, the initial

evolution along ring-planarization coordinates is needed to create an appropriate intermediate structure from which the predicted bonding changes can take place. Thus, we conclude that the reaction coordinate of COT is sequential. However, these results do not preclude the remaining "reactive" changes from proceeding in a concerted manner. In contrast, *the planar and near-planar ground states of CB and CHD allow for excited-*
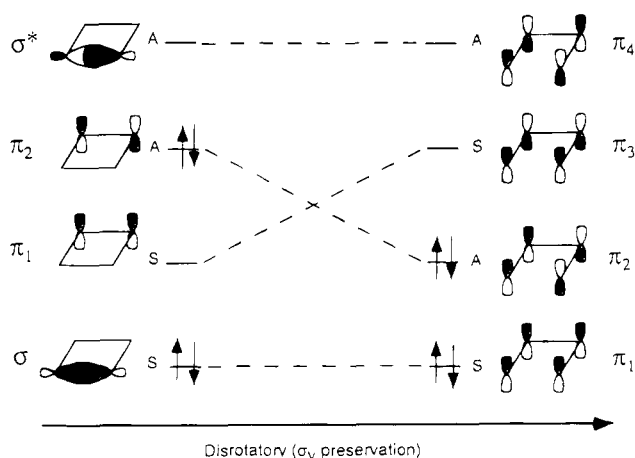
Pericyclic Photochemical Ring-Opening Reactions

Acc. Chem. Res., Vol. 28, No. 12, 1995 **501**

Disrotatory (σ_v preservation)

Figure 11. Orbital symmetry correlation diagram for the photochemical ring opening of CB. This figure depicts a doubly excited electronic configuration of CB which correlates directly with the ground state of the product.

state evolution along the Woodward–Hoffmann predicted stereochemical reaction coordinate immediately after excitation. Thus, these rearrangements have a concerted reaction mechanism. It should be noted that, in all treatments of pericyclic theory, the molecule in question is first reduced to its highest possible symmetry which involves assuming a planar molecule. This difference in excited-state dynamics suggests that atomic orbital overlap is an important factor in pericyclic photochemistry and could be an equivalent consideration for the analogous thermal reactions.

The role of the initially prepared excited state in these systems is to direct the reactant toward the portion of the potential energy surface where the majority of the pericyclic rearrangement occurs. In some cases the initial geometric motion is along the expected reaction coordinate (CB and CHD), and in other cases it is not (COT). *The short electronic-state lifetime for the initially prepared excited electronic state together with the 10–20 ps photoproduct appearance time on the ground-state surface indicates that it is in the lower lying $2A_1$ electronic state where the majority of the pericyclic rearrangement occurs.*[40,41,77]

Understanding the nature of the $2A_1$ state and how it plays its role in transforming reactant to photoproduct is obviously of great importance. Figure 11 depicts the doubly excited electronic configuration that is expected to contribute significantly to the low-lying $2A_1$ state in CB, where two electrons are elevated to the π_2 molecular orbital. This is the same molecular orbital that is singly occupied in states produced by one-photon excitation. This doubly excited state directly correlates to the ground-state photoproduct, and unlike the singly excited correlation diagram in Figure 2, the energy of the configuration is predicted to go *down* as the reaction proceeds. Hence the reaction is highly favorably from a pure symmetry point of view. This is a general feature of this electronic configuration for both cyclic and linear polyenes.

Theoretical calculations have anticipated the involvement of the $2A_1$ state in these reactions for decades.[15,78,79] These predictions were obtained by

calculating energies of excited states at positions that correlate with the expected ground-state trajectories for "allowed" and "forbidden" transformations. The result was that the $1B_2$ and $2A_1$ states rapidly crossed as the molecule moved along the reaction coordinate. The molecule would, after making the $1B_2$ to $2A_1$ transition, end up in a "well" on the $2A_1$ state that was located directly above a maximum in the ground-state potential. From this minimum the molecule could internally convert to the ground state to form photoproduct. In this one-dimensional picture, the $2A_1$ state and the ground $1A_1$ state cannot cross due to symmetry. Therefore, the transition between the excited 2A state and the ground 1A state must occur through an avoided curve crossing. While this transition may be unlikely because of the large energy gap between the two surfaces, this model has served for years as the best explanation for the pericyclic reaction.

Recent *ab initio* calculations by Robb, Bernardi, and Olivucci do not restrict the path followed on the $2A_1$ surface to only one dimension, and therefore they provide further insight into the possible dynamics on the $2A_1$ surface.[80] In these calculations, states of the same spin or spatial symmetry are not restricted by the "rule of noncrossing". For the simplest case of two coordinates, the two states will intersect at a point and the resulting energy plot will resemble two cones (one inverted on top of the other) connected through their vertexes. These conical intersections have been found to be a common feature in these calculations. In the specific example of CHD, after internal conversion from the $1B_2$ state to the $2A_1$ state, the excited CHD relaxes directly into the $2A_1$ minimum of the *all-cis*-1,3,5-hexatriene (*cis*-HT). A conical intersection is calculated to connect the $2A_1$ and $1A_1$ surfaces at a point near the *cis*-HT geometry.[81] At no point along this excited-state trajectory is there an area that could be described as an avoided curve crossing. From this $2A_1$ *cis*-HT well, the molecule must overcome an energy barrier of approximately 1 kcal/mol to reach the conical intersection with the ground state. This energy barrier correlates well with the observed 6 ps appearance time of *cis*-HT on the ground state.[77,82] In this picture, after passing through the conical intersection, the molecule arrives on the ground state and may either revert back to CHD or continue on to form ground-state *cis*-HT. Since the efficiency of going through a conical intersection is unity, the momentum of the molecule as it enters the conical intersection and the shape of the conical intersection itself determine whether the molecule continues on to photoproduct or back to reactant. In this mechanism, the *cis*-HT well on the $2A_1$ surface acts as a common intermediate in the photochemical transformation of CHD to *cis*-HT and *vice versa*.

Our experimental evidence directly implicates the involvement of the $2A_1$ state in pericyclic ring-opening photochemistry and demonstrates the very limited but

(77) Reid, P. J.; Wickham, S. D.; Mathies, R. A. *J. Phys. Chem.* **1992**, *96*, 5720–5724.

(78) Share, P. E.; Kompa, K. L.; Peyerimhoff, S. D.; Van Hemert, M. C. *Chem. Phys.* **1988**, *120*, 411–419.

(79) Grimbert, D.; Segal, G.; Devaquet, A. *J. Am. Chem. Soc.* **1975**, *97*, 6629–6632.

(80) (a) Bernardi, F.; Olivucci, M.; Robb, M. A. *Pure Appl. Chem.* **1995**, *67*, 17–24. (b) Robb, M. A.; Bernardi, F.; Olivucci, M. *Ibid.* **1995**, *67*, 783–789.

(81) Celani, P.; Ottani, S.; Olivucci, M.; Bernardi, F.; Robb, M. A. *J. Am. Chem. Soc.* **1994**, *116*, 10141–10151.

(82) Pullen, S.; Walker, L. A., II; Donovan, B.; Sension, R. J. *Chem. Phys. Lett.* **1995**, *242*, 415–420.

significant involvement of the $1B_2$ state. In fact, our work experimentally shows that the $1B_2$ state acts to "set up" the photochemical changes to occur on the $2A_1$ surface either through planarization to attain atomic orbital overlap or through initiation of the resulting stereochemistry. Since our experiments have not probed the internal conversion from the $2A_1$ surface to the $1A_1$ surface, we have no data on these structures. However, very recent femtosecond time-resolved absorption studies on CHD by Sension and co-workers have indicated that this internal conversion process occurs with a time constant of approximately 1 ps and is solvent independent.[82] These results are consistent with a near-barrierless reaction coordinate. At this time a conical intersection seems to be the most reasonable model of those presented to date, but a critical test of this model has yet to be performed.

Concluding Remarks

We have used resonance Raman intensities to investigate the ultrafast nuclear dynamics of photochemical electrocyclic ring-opening reactions. Although the initial excited states for these systems are

populated for only 10–30 fs, they play an important role in directing the photoexcited system to the appropriate region of the excited-state potential energy surface. Our results provide a new and more complete understanding of the initial nuclear dynamics that make up the reaction coordinate, the states responsible for directing the photochemical reactions, and their lifetimes. Of course, these results generate important new questions. At what energy is the $2A_1$ state located? What factors control the $1B_2$ to $2A_1$ and $2A_1$ to $1A_1$ transitions? In particular, are these transitions controlled by static internal conversion factors or are nonstationary vibrational states involved in the photochemistry as has been recently revealed in studies of visual pigment photochemistry?[83] Answering these challenging and interesting questions will make studies of photochemical pericyclic reactions valuable for years to come.

(83) Wang, Q.; Schoenlein, R. W.; Peteanu, L. A.; Mathies, R. A.; Shank, C. V. *Science* **1994**, *266*, 422–424.